Convergent close-coupling calculations of positron scattering on H^-

R. Utamuratov,* D. V. Fursa, A. S. Kadyrov, and I. Bray
Curtin Institute for Computation and Department of Physics and Astronomy, Curtin University, Perth, Western Australia 6102, Australia

(Received 18 June 2019; published 8 October 2019)

The convergent close-coupling method has been applied to positron scattering by the hydrogen negative ion. Convergence of the cross sections is achieved and internal consistency of the method is verified using both the single- and two-center approaches. Calculations were performed using accurate target wave functions obtained with the multicore approach. Obtained results for Ps formation and breakup cross sections are compared with previous calculations.

DOI: 10.1103/PhysRevA.100.042703

I. INTRODUCTION

Positron (e^+) collisions with the hydrogen negative ion (H^-) are particularly interesting due to the large cross section for creating positronium (Ps), a bound electron-positron state. Positrons are the most accessible antimatter particles with a wide range of practical applications [1,2]. The H^- ion is a unique system with just one bound state [3] and plays an important role in astrophysics [4,5].

Positron scattering by H^- has been studied by various theoretical methods over the past few decades. Rudge [6] calculated breakup from H^- by electron and positron impact within the first Born approximation (FBA). Chaudhuri [7] applied the FBA to calculate cross section of Ps formation in the ground state. Ghosh and Sinha [8,9] calculated single and double ionization of H^- by positron impact using the Coulomb-distorted eikonal approximation.

The most comprehensive study of the e^+-H^- collision system to date has been performed by McAlinden and coworkers [10] using the *R*-matrix close-coupling approach (RCCA), which included 22 states (combination of eigen- and pseudostates) of Ps and the ground state of H^-. They reported cross sections of breakup and Ps formation in the ground and a few excited states.

Other theoretical studies have investigated bound states of the e^+-H^- system [11–13]. Apart from finding the value of binding energies, another interesting question under debate was whether the e^+-H^- bound system is of a molecular type where the positron forms Ps with one of the electrons and then binds to H, or atomic type where the positron orbits the H^- ion. Analyses of its wave functions have indicated that the bond is of a molecular type [14,15]. However, other studies have concluded it is more of atomic type [16,17].

No experimental study of the e^+-H^- collision system has been undertaken due to challenges in preparing the H^- target. However, the recent progresses in positron scattering experiments combined with increased interest in this system by the Ps-beam experiments [18] and antihydrogen production studies [19] warrant more detailed theoretical studies of the e^+-H^- collisions.

In this paper we present application of the convergent close-coupling (CCC) method to the e^+-H^- collision system. The CCC method has been successfully applied to light and heavy projectile scattering from atomic and molecular targets [20–23] including positron scattering from two-electron atomic targets, namely, helium [24], magnesium [25], and metastable helium [26]. The negative charge of the H^- target presents an additional challenge [27] for calculations of rearrangement matrix elements. To that end we have recently developed a method [28] of calculating Ps-formation matrix elements that can be straightforwardly applied to charged targets.

II. METHOD

Formalism of the CCC method for the e^+-H^- collision system is quite similar to the positron-helium case given in detail in Refs. [24,26]. Here we give only a brief description.

The nonrelativistic Hamiltonian for the e^+-H^- system can be written as

$$H = H_0 + \frac{1}{r_0} - \frac{1}{r_1} - \frac{1}{r_2} + \frac{1}{|\boldsymbol{r}_1 - \boldsymbol{r}_2|} - \frac{1}{|\boldsymbol{r}_0 - \boldsymbol{r}_1|} - \frac{1}{|\boldsymbol{r}_0 - \boldsymbol{r}_2|}, \tag{1}$$

where

$$H_0 = -\tfrac{1}{2}\nabla_0^2 - \tfrac{1}{2}\nabla_1^2 - \tfrac{1}{2}\nabla_2^2 \tag{2}$$

is the free Hamiltonian of the positron and two electrons, positions of which are given by vectors $\boldsymbol{r}_0$, $\boldsymbol{r}_1$, and $\boldsymbol{r}_2$, respectively.

The total scattering wave function Ψ for the system satisfies the Schrödinger equation

$$(H - E)\Psi(\boldsymbol{r}_0, \boldsymbol{r}_1, \boldsymbol{r}_2) = 0, \tag{3}$$

where E is the total energy.

The positron-atom scattering system has two centers, one associated with the target atom and the other with Ps. The CCC approach to positron scattering is based on the expansion of the total wave function Ψ in terms of states of all

*r.utamuratov@curtin.edu.au

asymptotic channels

$$\Psi \approx \sum_{\alpha}^{N_\alpha} F_\alpha(\boldsymbol{r}_0)\psi_\alpha(\boldsymbol{r}_1,\boldsymbol{r}_2) + \sum_{\beta}^{N_\beta}\{G_\beta(\boldsymbol{R}_{01})\phi_{1s}(\boldsymbol{r}_2)\psi_\beta(\boldsymbol{\rho}_{01}) + G_\beta(\boldsymbol{R}_{02})\phi_{1s}(\boldsymbol{r}_1)\psi_\beta(\boldsymbol{\rho}_{02})\}, \quad (4)$$

where the indices α and β denote a full set of quantum numbers of the target and Ps states, respectively. The first term corresponds to expansion in terms of target wave functions ψ_α with expansion coefficients F_α. The second term corresponds to expansion in terms of the Ps states ψ_β with coefficients G_β. The N_α and N_β are the numbers of the atomic and Ps states, respectively. The function ϕ_{1s} describes the residual electron in H with assumption that it is left in the ground state after Ps formation. The vector $\boldsymbol{R}_{0j} = (\boldsymbol{r}_0 + \boldsymbol{r}_j)/2$ indicates the positions of the Ps center relative to the proton and $\boldsymbol{\rho}_{0j} = \boldsymbol{r}_0 - \boldsymbol{r}_j$ is the relative coordinate of Ps, $j = 1, 2$.

The target wave functions ψ_α are calculated using the configuration interaction expansion

$$\psi_\alpha = \sum_{ab} C^\alpha_{ab} \sum_{l_a,m_a,l_b,m_b} C^{lm}_{l_a m_a\, l_b m_b}\phi_a(\boldsymbol{r}_1)\phi_b(\boldsymbol{r}_2). \quad (5)$$

The configuration interaction coefficients

$$C^\alpha_{ab} = -1^{l_a+l_b-l} C^\alpha_{ba}$$

ensure antisymmetry of the wave functions and are obtained by diagonalizing the target Hamiltonian [29]. The single-particle basis functions ϕ are taken as

$$\phi_a(\boldsymbol{r}_1) = \frac{1}{r} R_{n_a l_a}(r) Y_{l_a m_a}(\hat{r}), \quad (6)$$

where $Y_{l_a m_a}$ are the spherical harmonics and $R_{n_a l_a}$ are radial basis functions which are taken as the square-integrable orthogonal Laguerre functions.

Using expansion (4), the Schrödinger equation (3) for the total wave function is transformed into momentum-space coupled-channel equations for the transition matrix elements, from which cross sections of various transitions can be obtained [24,30].

The single-center method, with $N_\alpha > 0$ and $N_\beta = 0$, is relatively straightforward as it only involves evaluation of direct transition matrix elements. Ps formation is not explicitly included, but may be treated to convergence together with ionization (real or virtual) by positive energy atomic pseudostates of large orbital angular momentum [31]. The two-center calculations of the e^+-H^- present a few computational challenges. One is that the calculations of Ps-formation matrix elements are particularly involved due to two-center integrals that contain the radial Coulomb wave functions. We apply the recently reported method of calculating Ps-formation matrix elements [28] that simplifies the calculations and facilitates its application to charged targets.

Another challenge in the two-center approach to the e^+-H^- collision system is calculations of matrix elements for Ps $\rightarrow$ Ps transitions including electron exchange between the Ps and the residual H atom. In this work we ignore such electron-exchange effects. The Ps $\rightarrow$ Ps transitions are secondary channels in the e^+-H^- collision system and therefore electron exchange between Ps and H is not expected to have a crucial effect on the integrated cross sections. This expectation is backed by our previous successful calculations of positron scattering from two or more electron targets (He [24], Mg [25], and H_2 [22]), where we also have omitted electron exchange between Ps and residual ions in calculations of the Ps-Ps transition matrix elements. The single-center CCC approach using fully symmetrized target wave functions does properly incorporate electron exchange. Therefore, by comparing the two- and single-center CCC results we can check the validity of the approximations as well as internal consistency [31] of the CCC method.

III. RESULTS

H^- is a two-electron system with only one bound state. The measured breakup ($H^- \rightarrow e^-$-H) energy is 0.7542 eV [32]. In this study of the e^+-H^- collisions we consider only the following main reaction channels:

$$\text{elastic: } e^+\text{-H}^- \rightarrow e^+\text{-H}^-,$$
$$\text{breakup: } e^+\text{-H}^- \rightarrow e^+\text{-}e^-\text{-H},$$
$$\text{Ps formation: } e^+\text{-H}^- \rightarrow \text{Ps-H}.$$

Other reactions such as a direct annihilation and breakup with excitation (of the residual hydrogen) are negligible for the energy range we consider. Because the H^- is a charged target, the angle-integrated elastic-scattering cross section is infinite. However, breakup and Ps-formation cross sections should have finite values, except near zero collision energies where the latter is predicted to have $1/E$ behavior [5].

The CCC method can be applied to the positron scattering problem within the single- and two-center approaches allowing for an internal consistency check of the method [31]. The single-center approach ($N_\alpha > 0$ and $N_\beta = 0$) is applicable to this system above the breakup threshold and can produce electron-loss (sum of breakup and Ps formation) cross sections. The two-center approach ($N_\alpha > 0$ and $N_\beta > 0$) allows calculations of the Ps-formation and breakup cross sections explicitly. By internal consistency we mean that the electron-loss cross section in the one-center calculation should be the same as the sum of Ps-formation and breakup cross sections arising in the two-center calculations.

The CCC method relies on convergence of observables of interest as a function of the increasing number of states (N_α and N_β) included in the multichannel expansion given in Eq. (4). For simplicity of presentation, we show the convergence study of the results separately for the single- and two-center approaches. The convergence studies are important in indicating the uncertainties associated with the calculations.

A. Single-center calculations

The single-center calculations are performed with different total number of target pseudostates, calculated as $N_\alpha = \sum_l^{l_{\max}} N_l$, by increasing the values of N_l for each $l \leqslant l_{\max}$. For simplicity we set the basis size for each value of orbital momentum as $N_l = N_0 - l$. To further simplify the convergence studies, we set the value of N_0 to 25. We have verified that $N_0 = 25$ was sufficient to achieve a good convergence of cross sections for each given value of $l_{\max}$. This allows us to concentrate on the convergence rate when the value of $l_{\max}$

TABLE I. Single-electron energies (in eV) of H^- used in the calculations.

n \ l	s	p	d	f
1	−0.736			
2	0.021	0.024		
3	0.084	0.071	0.036	
4	0.190	0.143	0.092	0.032
5	0.344	0.242	0.171	0.072
6	0.549	0.371	0.276	0.127
7	0.813	0.535	0.410	0.197
8	1.145	0.738	0.577	0.286
9	1.559	0.988	0.783	0.395
10	2.072	1.295	1.033	0.528

is systematically increased. The following list describes the basis types and their notations.

(a) A basis with $l_{\max} = 0$, $N_\alpha = 25$ is denoted as CCC(25_0, 0).

(b) A basis with $l_{\max} = 1$, $N_\alpha = 49$ is denoted as CCC(25_1, 0).

(c) A basis with $l_{\max} = 3$, $N_\alpha = 94$ is denoted as CCC(25_3, 0).

(d) A basis with $l_{\max} = 5$, $N_\alpha = 135$ is denoted as CCC(25_5, 0).

(e) A basis with $l_{\max} = 7$, $N_\alpha = 172$ is denoted as CCC(25_7, 0).

These bases produce accurate representation of the bound state of H^- and a sufficiently dense discretization of the continuum. Table I shows the lowest single-electron energies of pseudostates with $n \leqslant 10$ and orbital angular momenta values $l \leqslant 3$. The bound-state energy is 0.736 eV, which is within 2.4% of the experimental value of 0.754 eV [32]. The positive-energy state spectrum is dense at lower energies but gets more sparse for higher energies.

Dipole polarizability obtained by summing over the pseudostate spectrum is 215.14 and compares well with the value of $\alpha_d = 206.149$ obtained in accurate calculations of Bhatia and Drachman [33].

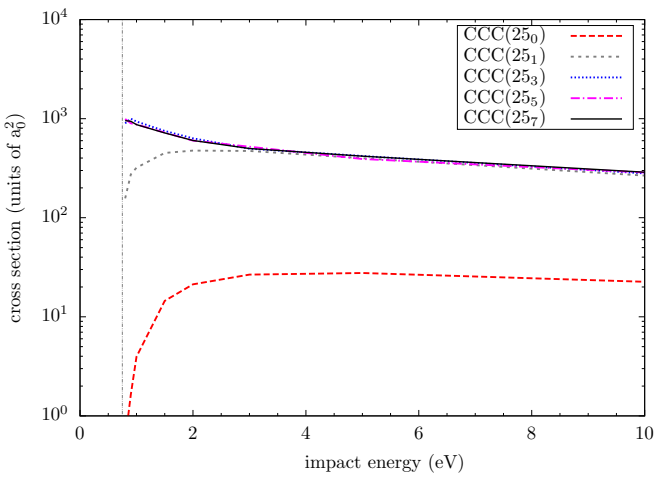

FIG. 1. Convergence of the electron-loss cross sections calculated within the single-center approach.

Since the target is charged, the integrated elastic scattering cross section is infinite. Therefore, in the absence of any target excited states, only measurable cross sections are breakup and Ps-formation ones, the sum of which is called the electron-loss cross section. In the single-center CCC method the electron-loss cross section is calculated as a sum of the cross sections for excitation of the positive-energy pseudostates.

The electron-loss cross sections calculated with different basis sizes are shown in Fig. 1. The cross sections rise rapidly from $l_{\max} = 0$ to $l_{\max} = 1$ at all energies. From $l_{\max} = 1$ to $l_{\max} = 3$ a noticeable change is found only below 3 eV impact energies. The results for $l_{\max} = 3$ are only slightly different from those for $l_{\max} = 5$ near the threshold. Good agreement of the results for $l_{\max} = 5$ and $l_{\max} = 7$ indicate that convergence with increasing $l_{\max}$ has been achieved.

B. Two-center calculations

The two-center calculations are performed with the fixed number of H^- states, $N_\alpha = 27$, which has $10s$, $9p$, and $8d$ pseudostates and convergence is checked by increasing the number of included Ps states. Ps states are generated with the basis size of $N_l = 5 - l$ and the first three states closely represent the $1s$, $2s$, and $2p$ eigenstates while others are pseudostates and $n > 3$ pseudostates have positive energies.

The following list describes the two-center basis types and their notations.

(a) A basis with $N_\alpha = 27$, $N_\beta = 1$ is denoted as CCC(10_2, 1).

(b) A basis with $N_\alpha = 27$, $N_\beta = 3$ is denoted as CCC(10_2, 3).

(c) A basis with $N_\alpha = 27$, $N_\beta = 6$ is denoted as CCC(10_2, 6).

(d) A basis with $N_\alpha = 27$, $N_\beta = 9$ is denoted as CCC(10_2, 9).

In addition to the above models, we also performed calculations with two more different models where the target wave functions are obtained in the frozen-core model. The first one is labeled as FC CCC(10_2, 6) and is used to check how the accuracy of the target wave functions affect the results. It includes the same number of basis states as in the model CCC(10_2, 6), but differs in the accuracy of the target wave functions. The second is labeled as FC CCC($1s$,18) and is used to compare with the RCCA calculations of McAlinden *et al.* [10] employing similar basis and target wave function. It includes the target ground state obtained within the frozen-core model and 18 Ps pseudostates (up to $7\bar{s}$, $7\bar{p}$, and $7\bar{d}$ states) obtained with the basis size of $N_l = 7 - l$. In these frozen-core models the target bound state energy is −0.362 eV, which is the same as in the RCCA [10] calculations.

Cross sections of Ps formation in bound states obtained with different Ps-basis types are shown in Fig. 2. The results of the CCC(10_2, 1) model, which has only the ground state of Ps, are lower than the others. Adding $2s$ and $2p$ states of Ps changes the results substantially, indicating the importance of Ps formation in these states. Further addition of Ps pseudostates, some of which have positive energy, has slightly reduced the values of the cross sections. This is expected behavior of bound-state cross sections due to coupling to positive-energy pseudostates. Almost identical results of the

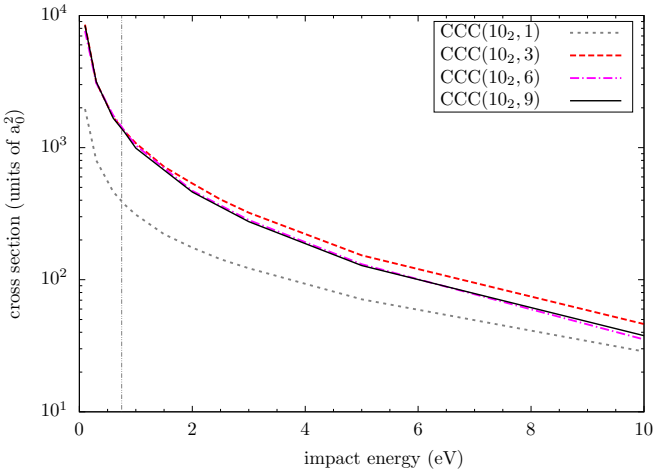

FIG. 2. Convergence of the two-center CCC calculations for the Ps-formation cross section.

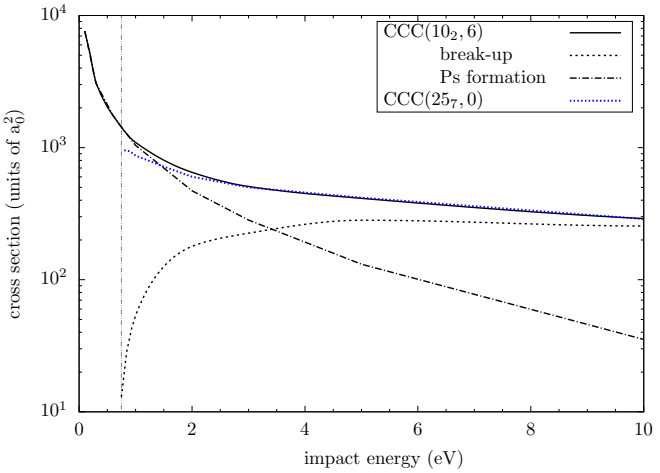

FIG. 4. Comparison of single- and two-center CCC calculations for electron-loss cross sections. The two-center CCC results for the contributions of Ps formation and breakup are also shown for comparison.

CCC(10_2, 6) and CCC(10_2, 9) models indicate that convergence has been achieved.

Figure 3 presents an electron-loss cross section obtained with the two-center expansions. The result of the CCC(10_2, 1) basis has a minima at the breakup energy threshold and is lower than other calculations. By adding Ps formation in $2s$ and $2p$ states the results have changed substantially at lower energies and the minima at the threshold have disappeared. Further addition of Ps pseudostates has only increased the cross section values at above 2 eV. Again, good agreement between the CCC(10_2, 6) and CCC(10_2, 9) results show convergence of the cross sections.

Comparison of the electron-loss cross sections obtained with the single- and two-center CCC methods is shown in Fig. 4. Good agreement between the two results confirm the internal consistency of the theory. A small difference just above the breakup threshold is expected due to slow convergence of the single-center results near the threshold.

This is related to a low number of open target-based pseudostates at low energies. Therefore, the single-center CCC for positron scattering is usually accurate at a few eV above the threshold.

The two-center CCC results for the electron-loss cross sections are calculated as a sum of the Ps formation and breakup cross sections. Between 0 and 3 eV the Ps formation is the main contributor and the breakup becomes the dominant contributor afterwards. Low value of the breakup cross sections near the breakup threshold is likely due to Ps being formed readily from slow moving electron and positrons.

Note that in the two-center calculations we have ignored electron exchange between Ps and H while evaluating the Ps-Ps transition matrix elements. However, close agreement of the single- and two-center results indicates that exchange terms in the Ps $\rightarrow$ Ps channels are small.

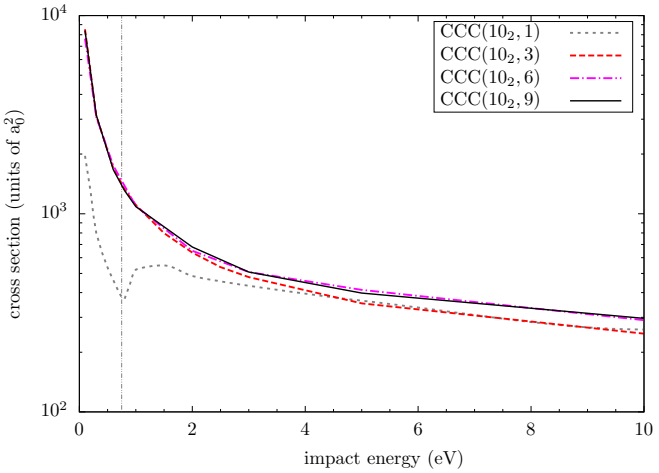

FIG. 3. Convergence of electron-loss cross sections calculated within the two-center CCC approach.

C. Comparison with the RCCA results and experimental data for electron impact

The RCCA method applied to the e^+-H^- collision system by McAlinden and co-workers [10] was the most comprehensive study to date. The RCCA calculations were performed using a two-center expansion which included 22 states (combination of eigen- and pseudostates) of Ps and the ground state of H^-. The wave function of H^- was obtained with the frozen-core type approach using only s functions which produced the single-electron detachment energy of 0.362 eV. In the scattering calculations, this energy was replaced by the correct ground-state energy of H^- in order to have the correct threshold energies.

Figure 5 compares various CCC-calculated cross sections for Ps formation in bound states with the RCCA results of McAlinden *et al.* [10]. Agreement between the two-center results marked as CCC(10_2, 6) and the RCCA is only in the shape and the energy dependence ($1/E$) of the Ps-formation cross sections at low energies. The FC CCC($1s$,18) compares better with the RCCA results, thereby indicating the importance of the better accuracy of the ground state obtained in the full CI calculations. The remaining difference can be attributed to different target and Ps wave functions used.

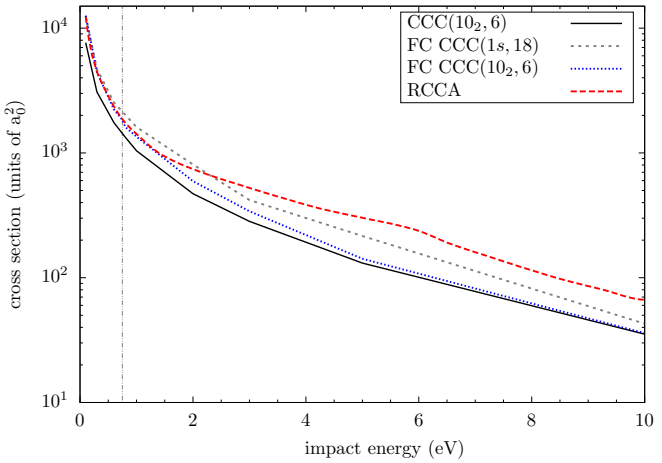

FIG. 5. Comparison of two-center results for total cross section of Ps formation in bound states.

Our calculations, not presented here, with different fall-off parameters of Ps pseudostate wave functions have shown that Ps-formation cross sections are very sensitive to a change in Ps pseudostates when the target positive-energy pseudostates are not included. When the latter are included, as in the present CCC two-center calculations, the results are less sensitive to Ps-basis parameters.

Comparison of the results from the CCC(10$_2$, 6) calculations with FC CCC(10$_2$, 6) shows how the quality of the target ground-state wave function affects the Ps-formation cross sections. At impact energies below 5 eV the frozen-core target wave function results FC CCC(10$_2$, 6) are considerably higher than the CCC(10$_2$, 6) results obtained with the accurate target ground-state wave function. But above 5 eV the difference between the two models gradually disappears.

Note that the Ps bases used in the RCCA and present calculations are somewhat different due to different ways used in obtaining them. However, the first three Ps states are sufficiently close to eigenstates in both cases. Therefore, in Fig. 6 we compare results for the sum of the cross sections for Ps formation in 1s, 2s, and 2p states. Results of the FC CCC(1s,18) model are lower than the RCCA results but both

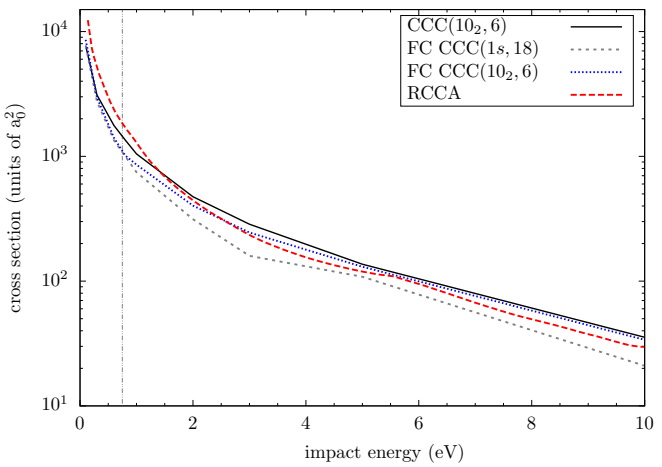

FIG. 6. Sum of cross sections of Ps formation in 1s, 2s, and 2p states.

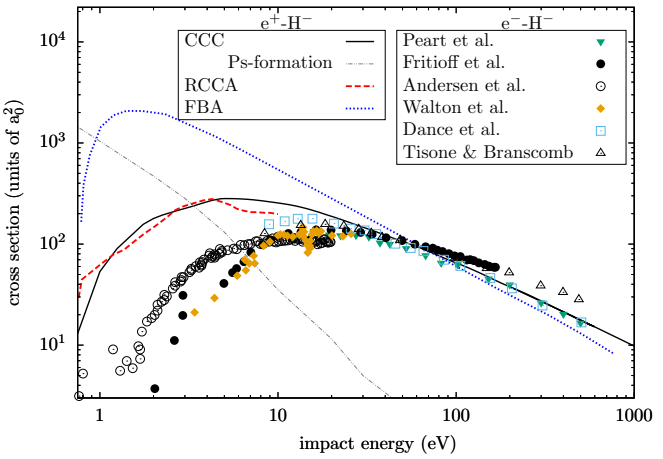

FIG. 7. Breakup cross sections for positron impact (present CCC, RCCA [10], and FBA [6]) and electron impact (experiment). The experimental data are due to Fritioff *et al.* [34], Peart *et al.* [35], Andersen *et al.* [36], Walton *et al.* [37], Dance *et al.* [38], and Tisone and Branscomb [39]. The CCC results for Ps formation are also shown for comparison.

have a similar shape. The two-center CCC results are also in good agreement with the RCCA ones. This agreement is quite surprising considering the different models and particularly different target wave functions used in the calculations. In this case, the FC CCC(10$_2$, 6) results are only slightly lower than the CCC(10$_2$, 6) results.

As seen in Fig. 5, the Ps-formation cross section falls off fast as impact energy increases. Therefore, at high enough energies, where Ps formation and electron exchange can be ignored, positrons should scatter similar to electrons. To check this, in Fig. 7 we compare the CCC, RCCA [10], and FBA [6] results for positron-impact breakup cross sections with experimental data for electron impact. The electron-impact measurements have been conducted over the past few decades starting in the early 1960s [34–39]. There are substantial differences between the different measurements. The CCC results for Ps formation are also presented for comparison. At energies above 50 eV, where Ps formation becomes negligible, the CCC results for positron impact are in good agreement with the measurements of Peart *et al.* [35] and Dance *et al.* [38]. At lower energies positron-induced breakup cross sections are much higher than for electrons due to the target having a negative charge that attracts positrons and repels electrons. The FBA calculations of Rudge [6] significantly overestimate the breakup cross sections below 50 eV highlighting the importance of close-coupling effects.

IV. SUMMARY

The CCC method has been applied to positron scattering from H$^-$. Convergence of results both in the single- and two-center approaches has been demonstrated. Electron exchange between the Ps and H atoms was neglected in calculations of the Ps-Ps matrix elements appearing in the two-center approach. Excellent agreement between the single- and two-center CCC results confirms the internal consistency and also justifies the validity of the approximation used in the

two-center CCC method. Comparison with the 22-state RCCA method shows some minor discrepancies which are attributed to differences in the methods and radial basis wave functions used in the calculations. The importance of the quality of the target ground-state wave function has been found to affect mostly the breakup cross sections, while Ps-formation cross sections are less sensitive provided there are a sufficient number of target pseudostates.

ACKNOWLEDGMENTS

The work was supported by the Australian Research Council. We are grateful for access to the Australian National Computing Infrastructure Facility and the Pawsey Supercomputing center in Western Australia. A.S.K. acknowledges partial support from the U.S. National Science Foundation under Award No. PHY-1415656.

[1] D. Bailey, D. Townsend, P. Valk, and M. Maisey, *Positron Emission Tomography* (Springer, London, 2005).
[2] A. David, G. Kögel, P. Sperr, and W. Triftshäuser, Phys. Rev. Lett. **87**, 067402 (2001).
[3] R. N. Hill, Phys. Rev. Lett. **38**, 643 (1977).
[4] S. Chandrasekhar and D. D. Elbert, Astrophys. J. **128**, 633 (1958).
[5] J. C. Straton and R. J. Drachman, Phys. Rev. A **44**, 7335 (1991).
[6] M. R. H. Rudge, Proc. Phys. Soc. **83**, 419 (1964).
[7] P. Chaudhuri, Braz. J. Phys. **31**, 1 (2001).
[8] D. Ghosh and C. Sinha, Phys. Rev. A **69**, 052717 (2004).
[9] D. Ghosh and C. Sinha, J. Phys. B **38**, 61 (2004).
[10] M. T. McAlinden, J. E. Blackwood, and H. R. J. Walters, Phys. Rev. A **65**, 032715 (2002).
[11] Y. K. Ho, Phys. Rev. A **17**, 1675 (1978).
[12] B. A P Page and P. A Fraser, J. Phys. B **7**, L389 (1974).
[13] M. Bromley, J. Mitroy, and G. Ryzhikh, Nucl. Instrum. Methods Phys. Res., B **171**, 47 (2000).
[14] M. W. J. Bromley and J. Mitroy, Phys. Rev. A **65**, 012505 (2001).
[15] P. Biswas and J. Darewych, Nucl. Instrum. Methods Phys. Res., B **192**, 138 (2002).
[16] Y. K. Ho, Phys. Rev. A **34**, 609 (1986).
[17] D. Bressanini and G. Morosi, J. Chem. Phys. **119**, 7037 (2003).
[18] S. Armitage, J. Beale, D. Leslie, and G. Laricchia, Nucl. Instrum. Methods Phys. Res., B **233**, 88 (2005).
[19] A. S. Kadyrov, A. V. Lugovskoy, R. Utamuratov, and I. Bray, Phys. Rev. A **87**, 060701(R) (2013).
[20] I. Bray, D. V. Fursa, A. S. Kadyrov, A. V. Lugovskoy, J. S. Savage, A. T. Stelbovics, R. Utamuratov, and M. C. Zammit, J. Phys. Conf. Ser. **488**, 012052 (2014).
[21] A. V. Lugovskoy, R. Utamuratov, A. S. Kadyrov, A. T. Stelbovics, and I. Bray, Phys. Rev. A **87**, 042708 (2013).
[22] R. Utamuratov, A. S. Kadyrov, D. V. Fursa, M. C. Zammit, and I. Bray, Phys. Rev. A **92**, 032707 (2015).
[23] R. Utamuratov, D. V. Fursa, N. Mori, A. S. Kadyrov, I. Bray, and M. C. Zammit, Phys. Rev. A **99**, 042705 (2019).
[24] R. Utamuratov, A. S. Kadyrov, D. V. Fursa, I. Bray, and A. T. Stelbovics, J. Phys. B **43**, 125203 (2010).
[25] R. Utamuratov, D. V. Fursa, A. S. Kadyrov, A. V. Lugovskoy, J. S. Savage, and I. Bray, Phys. Rev. A **86**, 062702 (2012).
[26] R. Utamuratov, A. S. Kadyrov, D. V. Fursa, I. Bray, and A. T. Stelbovics, Phys. Rev. A **82**, 042705 (2010).
[27] C. M. Rawlins, A. S. Kadyrov, and I. Bray, Phys. Rev. A **97**, 012707 (2018).
[28] R. Utamuratov, D. Fursa, A. Kadyrov, and I. Bray, Comput. Phys. Commun. **239**, 64 (2019).
[29] D. V. Fursa and I. Bray, Phys. Rev. A **52**, 1279 (1995).
[30] I. Bray and A. T. Stelbovics, Phys. Rev. A **46**, 6995 (1992).
[31] I. Bray, J. J. Bailey, D. V. Fursa, A. S. Kadyrov, and R. Utamuratov, Eur. Phys J. D **70**, 1 (2016).
[32] K. R. Lykke, K. K. Murray, and W. C. Lineberger, Phys. Rev. A **43**, 6104 (1991).
[33] A. K. Bhatia and R. J. Drachman, J. Phys. B **27**, 1299 (1994).
[34] K. Fritioff, J. Sandström, P. Andersson, D. Hanstorp, F. Hellberg, R. Thomas, W. Geppert, M. Larsson, F. Österdahl, G. F. Collins *et al.*, Phys. Rev. A **69**, 042707 (2004).
[35] B. Peart, D. S. Walton, and K. T. Dolder, J. Phys. B **3**, 1346 (1970).
[36] L. H. Andersen, D. Mathur, H. T. Schmidt, and L. Vejby-Christensen, Phys. Rev. Lett. **74**, 892 (1995).
[37] D. S. Walton, B. Peart, and K. T. Dolder, J. Phys. B **4**, 1343 (1971).
[38] D. F. Dance, M. F. A. Harrison, and R. D. Randell, Proc. R. Soc. London A **299**, 525 (1967).
[39] G. Tisone and L. M. Branscomb, Phys. Rev. Lett. **17**, 236 (1966).